Experimental studies on the development of water permeability of Portland cement paste blended with blast furnace slag

J.Zhou [1], G.Ye [1, 2], and K. van Breugel [1]

[1]Microlab, Delft University of Technology, Delft, the Netherlands; [2]Magnel Laboratory for Concrete Research, Ghent University, Ghent, Belgium

Abstract

It is well known that the properties of pore structure and permeability are important factors for the durability of cementitious materials. In this study, the pore structure and water permeability of Portland cement paste blended with 70% blast furnace slag (BFS) were investigated. Experimental results show that the water permeability of BFS cement varies from 2.96E-10 to 6.88E-12 depending on the water/binder (w/b) ratio and curing age. Among the properties of the pore structure of BFS cement pastes, the water permeability has a logarithmic relationship with the effective porosity and a linear relationship with the critical pore diameter.

1. Introduction

In recent years, the durability of concrete structures has become an important issue. In a given environment, the durability of cementitious materials mostly depends on the ease, which the harmful substances, like Cl^- ions, sulfate ions, and CO_2, penetrate into the concrete. Therefore, the microstructural properties, such as pore structure and permeability are the main factors, which determine the durability of concrete structures. In order to evaluate and model the durability of concrete structures made with BFS cement, a better understanding of the microstructural properties of cement pastes is necessary.

According to Zhou et al. [1], when the BFS content is below 70% by weight, the addition of BFS results in a fine pore structure with low connectivity. Many studies [2, 3] have reported that both BFS concrete and BFS cement paste have a low water permeability compared with Portland cement concrete and paste. This is because of the refinement of pore structure and the formation of additional hydrate precipitations in the gaps between adjacent particles except the hydration products formed around BFS and clinker particles [4, 5]. Ye [6] has studied the relationship between the pore structure and water permeability of Portland cement paste. He suggested that the pore size distribution, the critical pore diameter, and the effective porosity are crucial factors for the water permeability.

The aim of this paper is to experimentally investigate the development of the pore structure and water permeability of hardening BFS cement pastes. A relationship between pore structure and water permeability is found. In the experimental program, the pore structure of hardening pastes was measured by means of mercury intrusion porosity (MIP). The water permeability was measured on the basis of Darcy's law at stable flow through a saturated porous medium.

2. Materials and methods

2.1 Materials

In this study, CEM I 32.5R and BFS were mixed in the laboratory. Table 1 lists the chemical compositions of CEM I 32.5R and BFS. The mineral composition of CEM I 32.5R, calculated by modified Bogue equation [7], is 63.6% C_3S, 9.7% C_2S, 7.3% C_3A and 9.7% C_4AF. Blain values of CEM I 32.5R and BFS are 283 m^2/g and 420 m^2/g. Densities of CEM I 32.5R and BFS are 3.15 g/cm^3 and 2.85 g/cm^3 respectively. Two w/b ratios of 0.4 and 0.5 are chosen. BFS content in the Portland cement paste is 70% by weight.

Table 1: Chemical compositions of CEM I 32.5 R and BFS (The chemical composition of CEM I 32.5 R was obtained from the producer and that of BFS was measured by energy dispersive X-ray analysis).

Oxide	CEM I 32.5 R (%)	BFS (%)
CaO	64.1	40.77
SiO_2	20.1	35.44
Al_2O_3	4.8	12.98
Fe_2O_3	3.2	0.53
MgO	-	7.99
K_2O	0.52	0.49
Na_2O	0.28	0.21
SO_3	2.7	0.1
Cl^-	0.037	0.052

2.2 Mercury Intrusion Porosimetry (MIP)

MIP is used to investigate the pore structure of pastes. Although numerous researchers have reported the limitations of MIP test for the determination of the pore structure of cementitious materials [12], however, MIP is so far the most widely used method for this. By tracing the change the intrusion volume of mercury under progressive pressure, the total volume of pores, the effective volume of pores and the critical pore diameter can be determined.

2.2.1 Sample preparation

CEM I 32.5R and BFS were mixed with water by the HOBART® mixer. Subsequently, paste was cast into plastic bottles and rotated at a speed of 5 r/min for 24 hours in a room with the temperature of 20 ˚C. After sealed curing at 20 ˚C, the sample was split into small pieces around 1 g at 3, 7, 14 and 28 days. Then, the sample was dried by freeze-drying, because it minimizes the damage to the pore structure [6]. The drying procedure was described in details in [6].

2.2.2 MIP measurement

MIP measurement was carried out on the freeze-dried samples at the room with a temperature of 16˚C. The maximum mercury intrusion pressure is 210 MPa. The contact angle of 141˚ and the surface tension of 485 mN/m are used. According to Washburn equation [8], the information of the pores with the diameter larger than 0.0072 μm can be collected.

2.3 Water permeability

2.3.1 Principal of the water permeability test

The water permeability of cement paste was described by Darcy's law [9]. It states that the steady state rate of flow through a saturated porous medium is directly proportional to the hydraulic gradient Δ*h* (m), which is expressed as [6]:

$$Q = \frac{k r_{L} g}{m} \frac{A}{L} \Delta h \quad (10.1)$$

where, *Q* is the fluid velocity in unit time (m^3/s), *κ* is the intrinsic permeability (m^2), *g* is the gravitational acceleration (9.81 m/s^2), *μ* is dynamic viscosity of the fluid (Ns/m^2), *A* is the cross section area (m^2), and *L* is the thickness of the sample (m). The coefficient of water permeability K_w (m/s) can be written as:

$$K_w = \frac{QL}{A\Delta h} \quad (10.2)$$

Consequently, for a specimen with a given thickness and cross-section, the water permeability can be calculated with the data of the water fluid velocity and the hydraulic gradient.

2.3.2 Experimental set-up

Figures 1 and 2 show the water permeability apparatus schematically [6]. This system consists of a gas-pressure source, a gas/water reservoir, three parallel permeability cells, a computer controlling system, and a data acquisition system. The water fluid velocity in the form of the weight of come-out water is measured by a scale connected with computer. The hydraulic gradient is created by the external gas-pressure source. A pressure sensor connected with computer is used to measure the hydraulic gradient. The computer collected the data of water fluid velocity and hydraulic gradient every 0.01 hours.

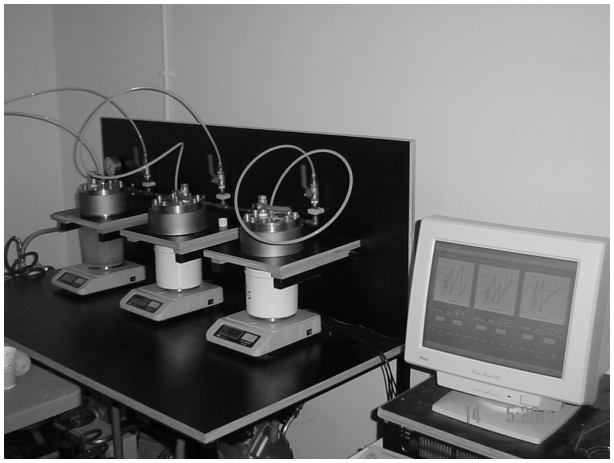

Figure 1: Picture of water permeability testing system [6].

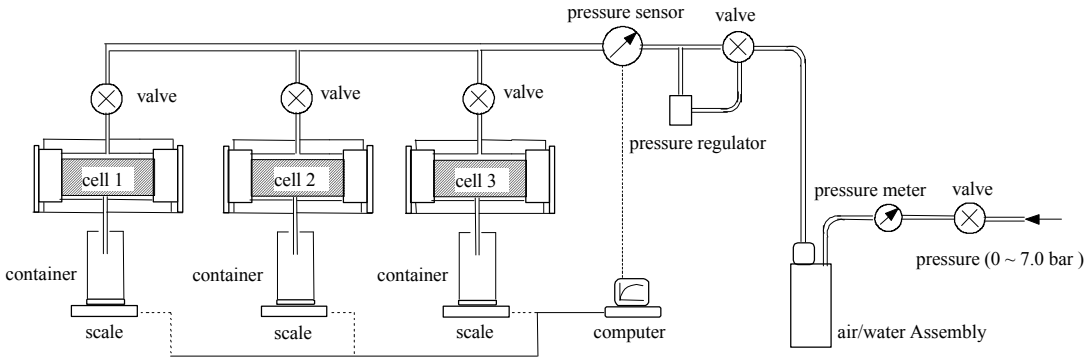

Figure 2: Water permeability testing system [6].

2.3.3 Experimental procedures

After mixed by the HOBART® mixer, paste was cast into a PVC cylinder with the inner diameter of 95 mm. Then, it was rotated in the speed of 5 r/min for 24 hours at 20 ˚C and cured under sealed condition at 20 ˚C. At certain curing age, 3 disks were cut from the whole sample with the thickness of around 10 mm. Before the water permeability test, the samples were saturated in calcium hydroxide solution for 6 hours.

After the saturation, the specimens were placed into the permeability cells. The bolts were fastened by an automatic screwdriver with constant twist. A hydrostatic pressure about 0.01 MPa was slowly applied to the cells. The valve was opened carefully in order to release air from the testing system. Then, the hydrostatic pressure was slowly increased to the desired value, which depends on the curing age. The values of 0.1, 0.2, 0.3 and 0.5 MPa were chosen for the sample at 3, 7, 14 and 28 days respectively. Each measurement was carried out until the steady-state flow.

The status of steady flow was determined by plotting the total weight of come-out water versus time. The interval was set to 0.01 hour. When the regression coefficient of the linearity of this curve during last 10 hours is

higher than 0.99, the water flow can be considered to be steady. In order to ensure good statistical confidence, the water permeability was calculated as the average of 3 samples prepared.

3. Result and discussion

3.1 Definition

In order to describe the pore structure of BFS cement pastes, the definition of some terms is given. According to Aligizaki [10], total porosity is defined as the fractional volume of pores with respect to the bulk volume of the material, and effective porosity is the fraction of only open and interconnecting pores with respect to the bulk volume of the material. Obviously, the effective porosity is an important factor to determine the permeability property of porous materials. In the cumulative porosity curve obtained from MIP test as shown in Figure 3, the total porosity is the total volume fraction of intruded mercury at the maximum pressure, and the effective porosity is the volume fraction of removed mercury during extrusion. Critical pore size is a term used to describe the pore size distribution. It corresponds to the steepest slope in cumulative porosity curves and to the peak in differential curves.

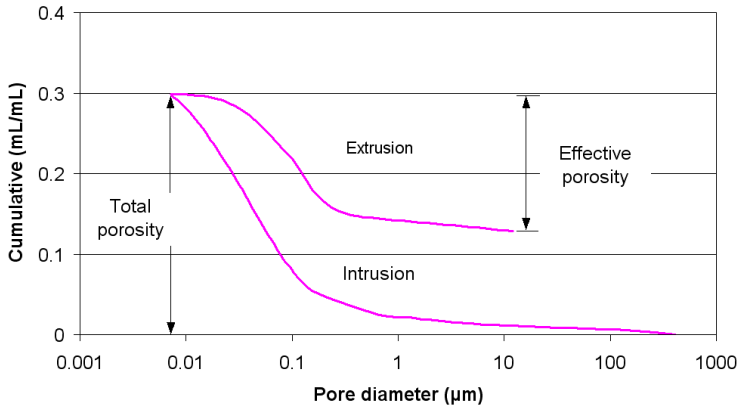

Figure 3: Cumulative porosity curve obtained from MIP test.

3.2 Water permeability

Table 2 gives the result of water permeability tests and its standard deviation. The standard deviation varies from 12% to 41%. According to Banthia and Mindess [11], considering the complicated experimental procedures, permeability coefficients with standard deviation less than 200% can be considered to be good results. This means that the results in this study are precise and the experimental set-up and procedures are reasonable.

Table 2: Water permeability coefficient of samples and its standard deviation.

Sample	Age (day)	Water permeability coefficient				
		Cell 1	Cell 2	Cell 3	Average	Standard deviation
CB-04-70	3	4.98E-11	4.11E-11	4.08E-11	4.39E-11	0.12
	7	1.94E-11	1.47E-11	2.60E-11	2.00E-11	0.28
	14	1.30E-11	5.58E-12	9.08E-12	9.23E-12	0.40
	28	9.51E-12	4.34E-12	6.79E-12	6.88E-12	0.38
CB-05-70	3	2.72E-10	2.25E-10	3.91E-10	2.96E-10	0.29
	7	5.71E-11	8.14E-11	7.44E-11	7.10E-11	0.18
	14	1.62E-11	2.03E-11	1.78E-11	1.81E-11	0.12
	28	7.62E-12	1.79E-11	1.20E-11	1.25E-11	0.41

Figure 4 plots the water permeability coefficient of BFS cement pastes with 70% BFS at 3, 7, 14 and 28 days. In the first 28 days, the water permeability coefficient of samples with higher w/b ratio is always higher than that of samples with lower w/b ratio. The difference of the water permeability coefficient between samples with varying w/b ratios becomes small, as curing age increases. In the first 7 days the water permeability coefficient decreases quickly, and then the decrease becomes slow. At early age, fast hydration results in the quick decrease in the amount and diameter of pores and thus the quick decrease in the water permeability. This can be confirmed by the development of pore structure as shown in Figures 5 and 6. As the curing age increases, both the total and effective porosity decrease, and the pore size becomes smaller. This means that the channel, which contributes to the transport of water fluids, becomes more discontinuous and narrower gradually. Therefore, it is more difficult for water to transport through it.

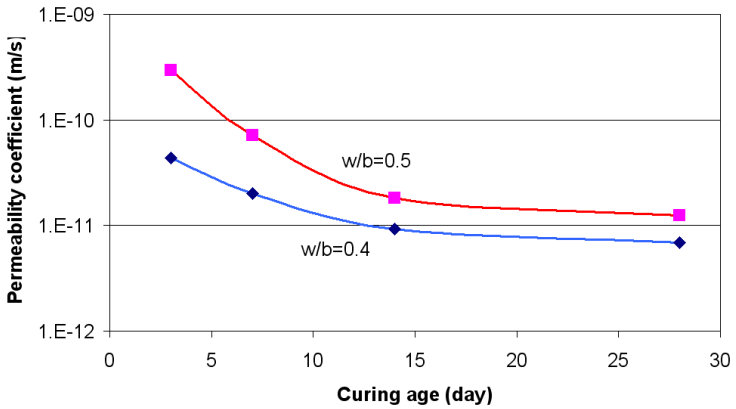

Figure 4: Water permeability coefficient of BFS cement pastes.

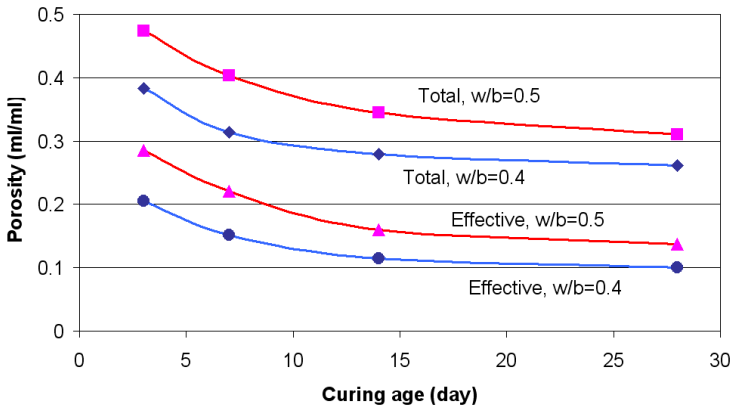

Figure 5: Porosity of BFS cement pastes with the w/b ratios of 0.4 and 0.5 at 3,7, 14 and 28 days.

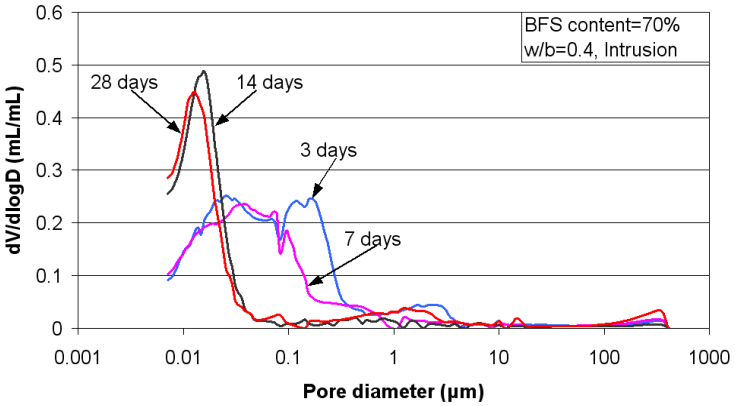

(a) Pore size distribution by mercury intrusion

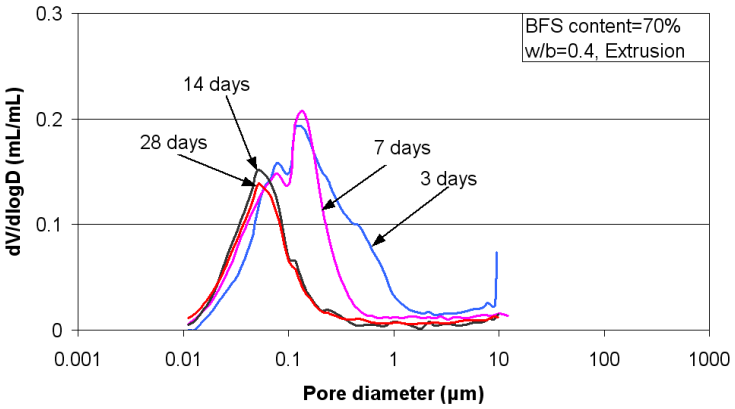

(b) Pore size distribution by mercury extrusion

Figure 6: Pore size distribution of BFS cement pastes with the w/b ratio of 0.4 at 3, 7, 14 and 28 days determined by mercury intrusion and extrusion.

3.3 Relationship between water permeability and pore structure

Figure 7 shows that the water permeability has a logarithmic relationship with the total and effective porosities. Compared with the total porosity, the relationship between the water permeability and the effective porosity is better. This confirms that effective pore system is more crucial for the transport properties of hardening cement pastes. In the hardening cement pastes, not all pores interconnect and contribute to the transport of water fluids. In other words, if the pores are discontinuous or ineffective to the transport of water fluids, although the total porosity is high, the water permeability is low. Hence, in addition to the porosity, the connectivity of pores in hardening cement pastes is also very important for the water permeability.

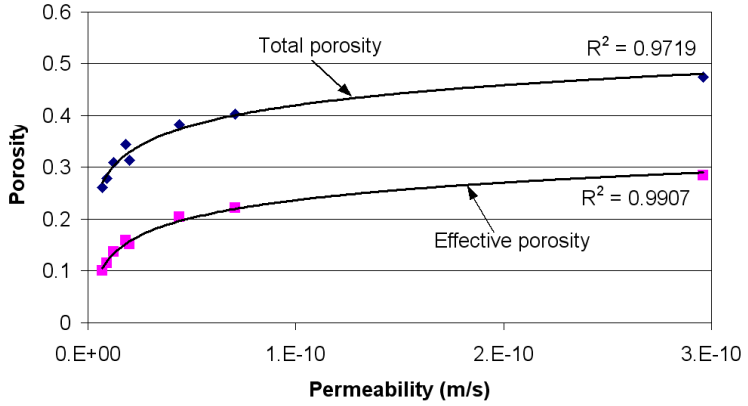

Figure 7: Relationship between the water permeability and the total and effective porosities.

Pore size distribution is another important property of the pore structure in cement pastes. Figure 8 shows the pore size distribution of cement pastes with the w/b ratio of 0.4 at 7days and the w/b ratio of 0.5 at 14 days, which have the water permeability coefficients of 2.00E-11 m/s and 1.81E-11 m/s respectively. The water permeability of the former one is slightly higher than that of the latter one, although the total porosity of the former one is 10% less than that of the latter one. However, they have the similar pore size distribution, especially the “effective pore size distribution” obtained from extrusion procedure. This implies that the pore size distribution, particularly “effective pore size distribution”, also has an influence on the transport properties of hardening cement pastes. Figure 9 shows that the water permeability has a good quadric relationship to the critical pore size obtained from extrusion procedure, which is named as “effective critical pore size”.

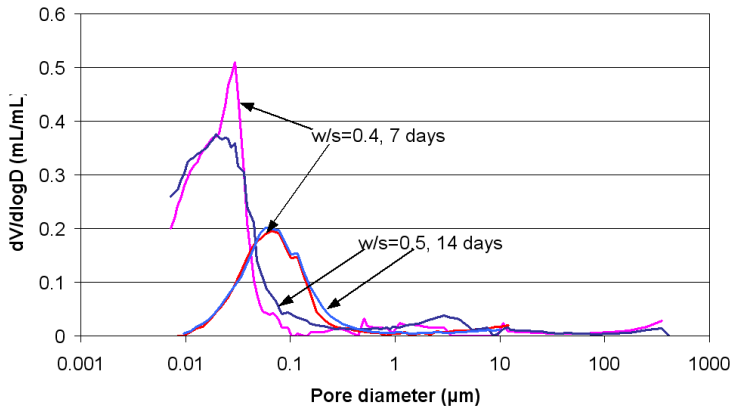

Figure 8: Pore size distribution of BFS cement pastes with the w/b ratio of 0.4 at 7days and the w/b ratio of 0.5 at 28 days.

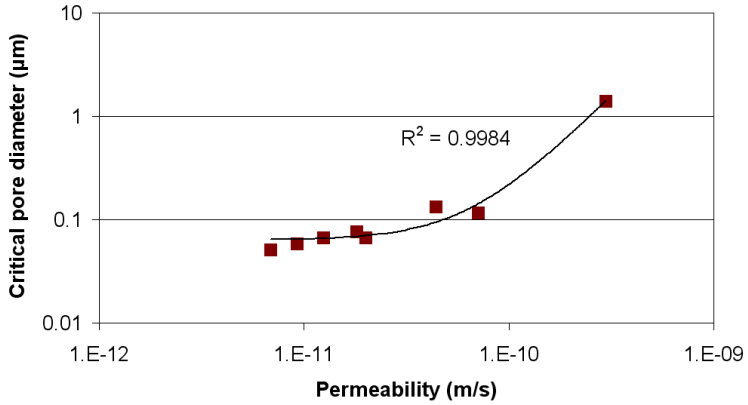

Figure 9: Relationship between water permeability and critical pore diameter.

4. Conclusions

The experimental results indicate that the experimental set-up and procedures are reasonable. The water permeability of Portland cement paste with 70% BFS varies from 2.96E-10 to 6.88E-12 depending on the w/b ratio and curing age. Among the properties of the pore structure of cement paste, effective pore system is more crucial for the water permeability.

References

[1] J. Zhou, G. Ye, K. van Breugel, Hydration process and pore structure of Portland cement paste blended with blast furnace slag, in Proc. of the 6th International Symposium on Cement and Concrete, September 19-22, Xian, China, 2006.

[2] C. M. Reeves, The use of GGBFS to produce durable concrete, in Improvement of Concrete Durability, Thomas Telford, London, 1985, pp. 59-76.
[3] R. D. Hootton, Permeability and pore structure of cement pastes containing fly ash, slag and silica fume, in Blended Cements, Ed. G. Frohnsdorf, ASTM SP-897, Philadelphia, 1986, pp. 128-143.
[4] R. F. Feldman, Significance of porosity measurements of blended cement performance, in 'Fly Ash, Silica Fume, Slag and other Mineral By-Products in Concrete', SP-79, ACI, Detroit, MI, 1983, pp. 415-433.
[5] R. Bakker, On the cause of increased resistance of concrete made from blastfurnace cement to the alkali-silica reaction and to sulphate corrosion, DSc thesis, Faculty of Mining and Metallurgy, R. W. T. H. Aachen, 1980, pp.94.
[6] G. Ye, The microstructure and permeability of cementitious materials, PhD thesis, Delft university press, Delft, the Netherlands, 2003.
[7] H. W. F. Taylor, Modification of the Bogue calculation, Adv. Cem. Res. 2 (6) (1989) 73-78.
[8] E.W. Washburn, in Proc. The National Academy of Sciences, PNASA, 7-21.
[9] E. J. Garboczi, Permeability, diffusivity, and microstructural parameters: a critical review, Cem. Concr. Res. 20 (1990) 591-601.
[10] K. K. Aligizaki, Pore structure of cement-based materials, Taylor & Francis, London, 2006.
[11] N. Banthia and S. Mindess, Permeability measurements on cement paste, Proc. Material Research Society Symposium, vol. 137, 1988, pp. 173-178.
[12] S. Diamond, Mercury porosimetry: an inappropriate method for the measurement of pore size distributions in cement-based materials, Cem Concr Res 30 (10) (2000) 1517-1525.